Chapter 8

FORMATION AND PROPERTIES OF CU-ZR-AG BULK METALLIC GLASSES

Starting from the two binary bulk-glass formers in the Cu-Zr system, we systematically investigated the compositional dependence of glass formation, thermal, elastic, and mechanical properties in the Cu-Zr-Ag ternary alloys. Both $Cu_{(50-x)}Zr_{50}Ag_x$ *and* $Cu_{(64-x)}Zr_{36}Ag_x$ *series alloys show a good combination of high glass-forming ability and high Poisson's ratio. However, compressive plastic deformation was only observed in* $Cu_{(50-x)}Zr_{50}Ag_x$ *series and the possible mechanism underneath is discussed.*

8.1. Introduction

Bulk metallic glasses (BMGs) have acquired significant attention from scientific and technological view points in the past twenty years [1, 2]. BMGs usually show high strength, large elastic strain limit, and excellent wear and corrosion resistances along with other remarkable engineering properties. Researchers have developed families of binary and multi-component systems to be BMG formers [3-12], among which highly processable Zr-based BMGs (Vitreloy series) have been utilized commercially to produce items such as sporting goods and electronic casings [3, 13].

Plenty of evidence has been shown that the ductile behavior of BMGs is closely related to their Poisson's ratio [14-18]. Lind, Duan, and Johnson investigated the isoconfigurational elastic constants and liquid fragility of a Zr-based BMG (Vitreloy 4) and discovered that the shear modulus, G, shows a strong reversible dependence on the specific configurational potential energy of the equilibrium liquid [19]. Such a strong configurational dependence of G in the liquid state is directly related to viscosity and fragility of the liquid, which has been also validated by molecular dynamics simulations [20, 21].

The glass-forming ability (GFA), rheological, and mechanical properties of BMGs have been extensively studied in different glass-forming systems. Previous literature indicates that highly processable Vitreloy BMGs tend to show rather strong liquid behaviors [22-24]. Recently it was discovered that Cu-Zr binary alloys, which can be cast into bulk amorphous structures with rod diameters up to 2 mm [8, 20, 25], show relatively fragile behaviors in viscosity [26]. Therefore, it is believed that there exists a balance point between GFA and fragility, which can be utilized to design tough bulk amorphous alloy systems.

Cu-Zr-based BMGs have received much attention since the binary $Cu_{64}Zr_{36}$ and $Cu_{46}Zr_{54}$ were reported to form bulk glassy alloys in 2004 *[8, 11, 20]*. Shortly after, the first Cu-Zr-based $Cu_{46}Zr_{42}Al_7Y_5$ glassy rods with diameters of 1 cm have been synthesized [8]. Dramatic compressive ductility was observed in the $Cu_{47.5}Zr_{47.5}Al_5$ alloy and the $Cu_{50}Zr_{50}$ alloy and was attributed to the unique structure correlated to atomic scale inhomogeneity *[27, 28]*. It was also found that the addition of Ag remarkably improved the glass-forming ability of Mg-Cu-Gd, Cu-Zr-Al, and Cu-Zr-Ti alloy systems [29-33]. Although bulk glass

formation and phase separation in the Cu-Zr-Ag system was reported already [34-36], we utilized a completely different approach in this work to study the compositional effect on elastic behaviors of Cu-Zr-Ag glassy alloys in an effort to further understand the relationship among Possion's ratio, fragility, and GFA. Recently the shear modulus, G, and Poisson's ratio, ν, are found to be very sensitive to composition changes in the Cu-Zr-Be ternary alloy system [37]. Here, starting from the two bulk glass formers in the Cu-Zr binary alloy system, $Cu_{64}Zr_{36,}$ and $Cu_{50}Zr_{50}$, we systematically studied the effect of Ag addition on glassy forming ability, and thermal properties in Cu-Zr-Ag bulk-glass- forming alloys, and investigated the compositional dependence of elastic properties and mechanical properties.

8.2. Experimental

For a complete description of sample preparation, characterization, and elastic property measurement details, please refer to Chapter 6.2. Cylindrical rods (2 mm in diameter and 4 mm in height) were used to measure mechanical properties of the Cu-Zr-Ag bulk glassy alloy on Instron testing machine at a strain rate of 1×10^{-4} s^{-1}. Before these mechanical tests, both ends of each specimen were examined with X-ray to make sure that the rod was fully amorphous.

8.3. Results and Discussions

Considering the chemical similarity of Cu and Ag, we systematically studied the effect of Ag addition on glass formation, thermal behavior, and elastic properties in Cu-Zr-Ag alloy system by always fixing the Zr concentration. We first examined glass formation in the $Cu_{(50-x)}Zr_{50}Ag_x$ series with the Zr content fixed at 50%, where x is 2, 5, 7, 10, and 12%. Figure 8.1 shows the X-ray diffraction patterns of amorphous 4 mm rod of $Cu_{45}Zr_{50}Ag_5$, 4 mm rod of $Cu_{43}Zr_{50}Ag_7$, 5 mm rod of $Cu_{40}Zr_{50}Ag_{10}$, and 7 mm rod of $Cu_{43}Zr_{40}Ag_7Ti_{10}$. It can be seen that the patterns of all the samples consist of only a series of broad diffraction maxima without detectable Bragg peaks. The DSC scans of the above four metallic glasses ($Cu_{45}Zr_{50}Ag_5$, $Cu_{43}Zr_{50}Ag_7$, $Cu_{40}Zr_{50}Ag_{10}$, and $Cu_{43}Zr_{40}Ag_7Ti_{10}$) are shown in Figure 8.2. Upon heating, these amorphous alloys exhibit a clear endothermic glass transition followed by one single or a series of exothermic events characteristic of crystallization. Clearly, fully glassy rods up to 7 mm diameter are formed with addition of 10% Ti to replace Zr in the ternary $Cu_{43}Zr_{50}Ag_7$ bulk amorphous alloy.

A summary of thermal and elastic properties of representative glassy alloys in the Cu-Zr binary, the Cu-Zr-Ag system, and two modified Cu-Zr-Ag-Ti(In) alloys is listed in Table 8.1. It also presents the casting diameter of fully amorphous rods of different compositions. The variations of supercooled liquid region, ΔT, ($\Delta T = T_x - T_g$, in which T_x is the onset temperature of the first crystallization event and T_g is the glass-transition temperature) and reduced glass-transition temperature T_{rg} ($T_{rg} = T_g/T_l$, where T_l is the liquidus temperature) are calculated. Elastic properties of these glassy alloys were measured and shear modulus,

G, bulk modulus, B, Young's modulus, Y, and Poisson's ratio, ν, are calculated and presented for comparison.

The binary $Cu_{50}Zr_{50}$ alloy is known to form bulk glassy rods of 2 mm in diameter by the copper mold casting method. The alloying effect of 2% Ag is minor and does not change T_g, T_x, and T_l very much. When Ag content is increased to 5 ~ 7%, 4 mm fully amorphous rods could be successfully obtained. With 10 %Ag, the GFA was improved to 5 mm. Once Ag is greater than 12%, the casting diameter of fully glassy rods is limited to 4 mm or less. Apparently, $Cu_{40}Zr_{50}Ag_{10}$ is the best glass former in the $Cu_{(50-x)}Zr_{50}Ag_x$ series. When a fourth element, Ti or In, is introduced, the GFA could be improved further. Fully glassy rods up to 7 mm in diameter are formed by the addition of 10% Ti into the ternary base $Cu_{43}Zr_{50}Ag_7$ alloy.

Table 8.1. Thermal and elastic properties of representative $Cu_{(50-x)}Zr_{50}Ag_x$ bulk glassy alloys.

Materials	d (mm)	T_g (K)	T_x (K)	T_l (K)	ΔT (K)	T_g/T_l	G (GPa)	B (GPa)	Y (GPa)	ν
$Cu_{50}Zr_{50}$	2	670	717	1208	47	0.55	30.0	119.9	83.2	0.384
$Cu_{48}Zr_{50}Ag_2$	2	668	719	1192	51	0.56	31.5	121.3	87.2	0.380
$Cu_{45}Zr_{50}Ag_5$	4	669	728	1188	59	0.56	31.5	120.0	87.0	0.379
$Cu_{43}Zr_{50}Ag_7$	4	669	727	1171	58	0.57	32.8	124.7	90.5	0.379
$Cu_{40}Zr_{50}Ag_{10}$	5	667	733	1177	66	0.57	31.6	117.2	87.0	0.376
$Cu_{38}Zr_{50}Ag_{12}$	4	663	734	1187	71	0.56	31.1	119.0	85.8	0.380
$Cu_{43}Zr_{43}Ag_7Ti_7$	5	670	714	1118	44	0.60	32.4	116.7	89.0	0.373
$Cu_{43}Zr_{43}Ag_7In_7$	5	704	748	1135	44	0.62	34.8	119.4	95.2	0.367

Table 8.2. Thermal and elastic properties of representative $Cu_{(64-x)}Zr_{36}Ag_x$ bulk glassy alloys.

Materials	d (mm)	T_g (K)	T_x (K)	T_l (K)	ΔT (K)	T_g/T_l	G (GPa)	B (GPa)	Y (GPa)	ν
$Cu_{64}Zr_{36}$	2	787	833	1230	46	0.64	34	104.3	92.0	0.352
$Cu_{57}Zr_{36}Ag_7$	4	712	755	1156	43	0.62	35.8	130.5	98.3	0.375
$Cu_{54}Zr_{36}Ag_{10}$	6	719	759	1146	40	0.63	35.2	124.8	96.4	0.371

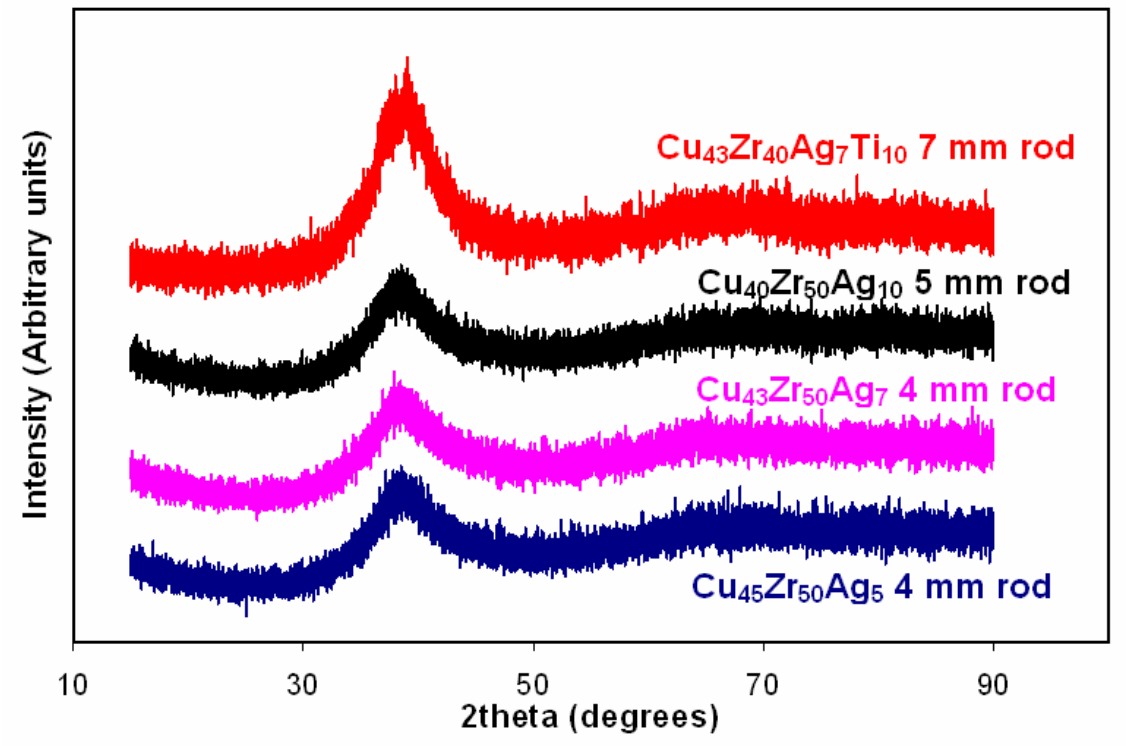

Figure 8.1. X-ray patterns of amorphous 4 mm rod of $Cu_{45}Zr_{50}Ag_5$, 4 mm rod of $Cu_{43}Zr_{50}Ag_7$, 5 mm rod of $Cu_{40}Zr_{50}Ag_{10}$, and 7 mm rod of $Cu_{43}Zr_{40}Ag_7Ti_{10}$ prepared by the copper mold casting method.

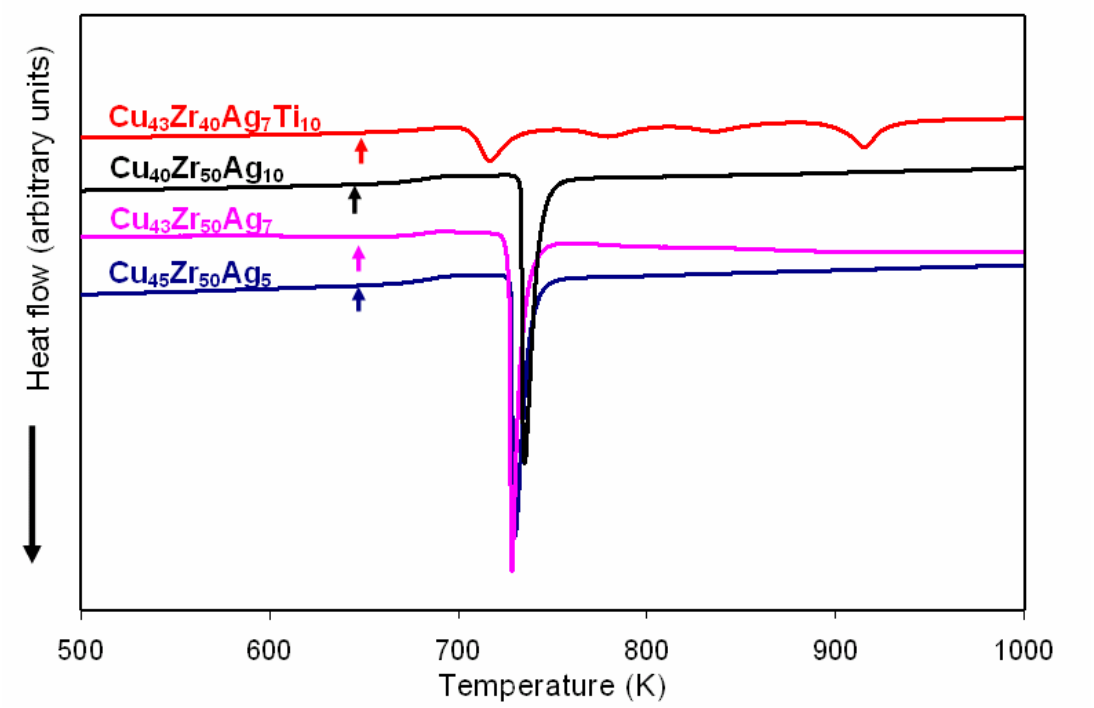

Figure 8.2. DSC scans of the amorphous $Cu_{45}Zr_{50}Ag_5$, $Cu_{43}Zr_{50}Ag_7$, $Cu_{40}Zr_{50}Ag_{10}$, and $Cu_{43}Zr_{40}Ag_7$-Ti_{10} alloys at a constant heating rate of 0.33 K/s. The marked arrows represent the glass transition temperatures.

It can be seen clearly from Table 8.1 that the addition of Ag increases the crystallization temperatures, stabilizes the supercooled liquids, and therefore benefits the GFA. With 10% Ag, ΔT is enlarged to 66 K compared to 47 K of the original $Cu_{50}Zr_{50}$ binary alloy. The second effect of Ag is to decrease the liquidus temperatures remarkably. The $Cu_{50}Zr_{50}$ binary alloy has a rather high T_l of 1208 K. When 7% Ag is added, the ternary $Cu_{43}Zr_{50}Ag_7$ shows a lower T_l of 1171 K. With another 7% of Ti and In, the quaternary $Cu_{43}Zr_{43}Ag_7Ti_7$ and $Cu_{43}Zr_{43}Ag_7Ti_7$ show even lower T_l of 1118 K and 1135 K, respectively. Thus, the alloying effect of Ag, Ti, and In brings the compositions into deeper eutectic and improves the GFA.

We then started from the binary $Cu_{64}Zr_{36}$ BMG and systematically studied the compositional dependence of glass formation, thermal, and elastic properties for the $Cu_{(64-x)}Zr_{36}Ag_x$ series alloys. X-ray patterns of different sizes of cast rods for different alloy compositions and the corresponding DSC scan curves are shown in Figure 8.3 and Figure 8.4, respectively. Thermal and elastic properties of $Cu_{(64-x)}Zr_{36}Ag_x$ series were evaluated and listed in Table 8.2. We notice that with 4% Ag addition, 3 mm fully amorphous cast rod of $Cu_{60}Zr_{36}Ag_4$ is not achievable, although a strong glassy background exists. When more Ag was added to the base alloy $Cu_{64}Zr_{36}$, the GFA of $Cu_{57}Zr_{36}Ag_7$ and $Cu_{54}Zr_{36}Ag_{10}$ are increased to 4 mm and 6 mm, respectively. Even if Ag is greater than 12%, the GFA could not exceed 7 mm, indicating that the best glass former is located around $Cu_{54}Zr_{36}Ag_{10}$. However, up to 8 mm glassy rods of the quaternary $Cu_{49}Zr_{36}Ag_{10}Ti_5$ alloy could be easily formed.

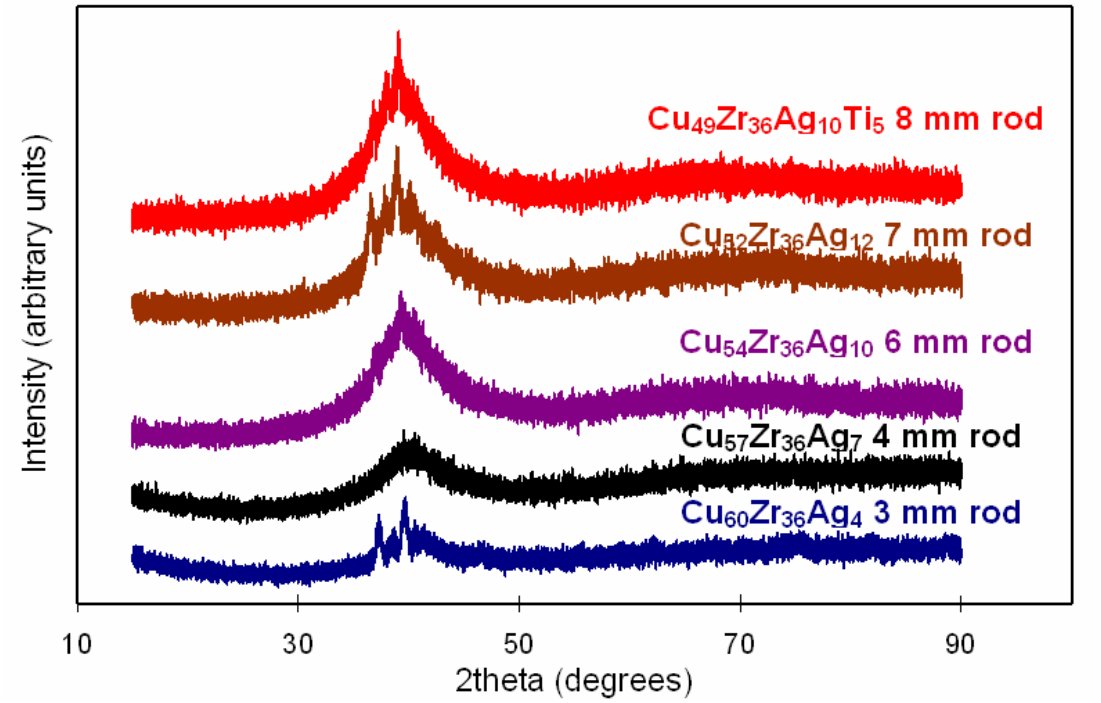

Figure 8.3. X-ray patterns of 3 mm cast rod of $Cu_{60}Zr_{36}Ag_4$, 4 mm glassy rod of $Cu_{57}Zr_{36}Ag_7$, 6 mm glassy rod of $Cu_{54}Zr_{36}Ag_{10}$, 7 mm cast rod of $Cu_{52}Zr_{36}Ag_{12}$, and 8 mm rod of $Cu_{49}Zr_{36}Ag_{10}Ti_5$.

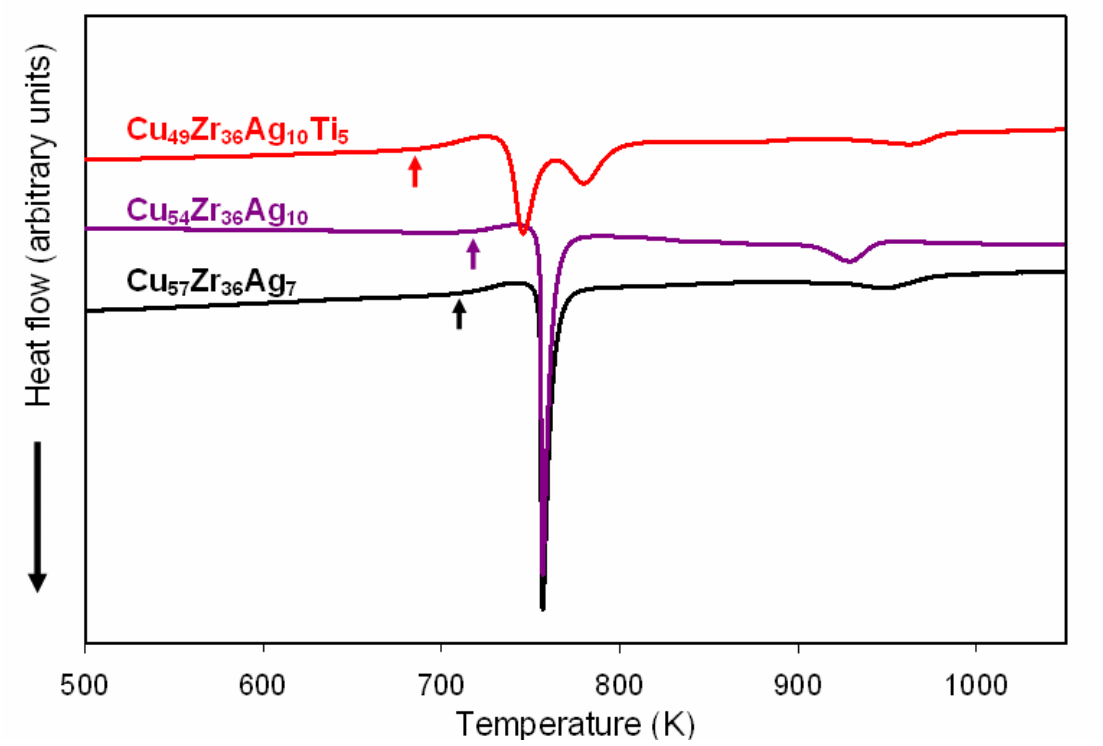

Figure 8.4. DSC scans of the amorphous $Cu_{57}Zr_{36}Ag_7$, $Cu_{54}Zr_{36}Ag_{10}$, and $Cu_{49}Zr_{36}Ag_{10}Ti_5$ alloys at a constant heating rate of 0.33 K/s. The marked arrows represent the glass transition temperatures.

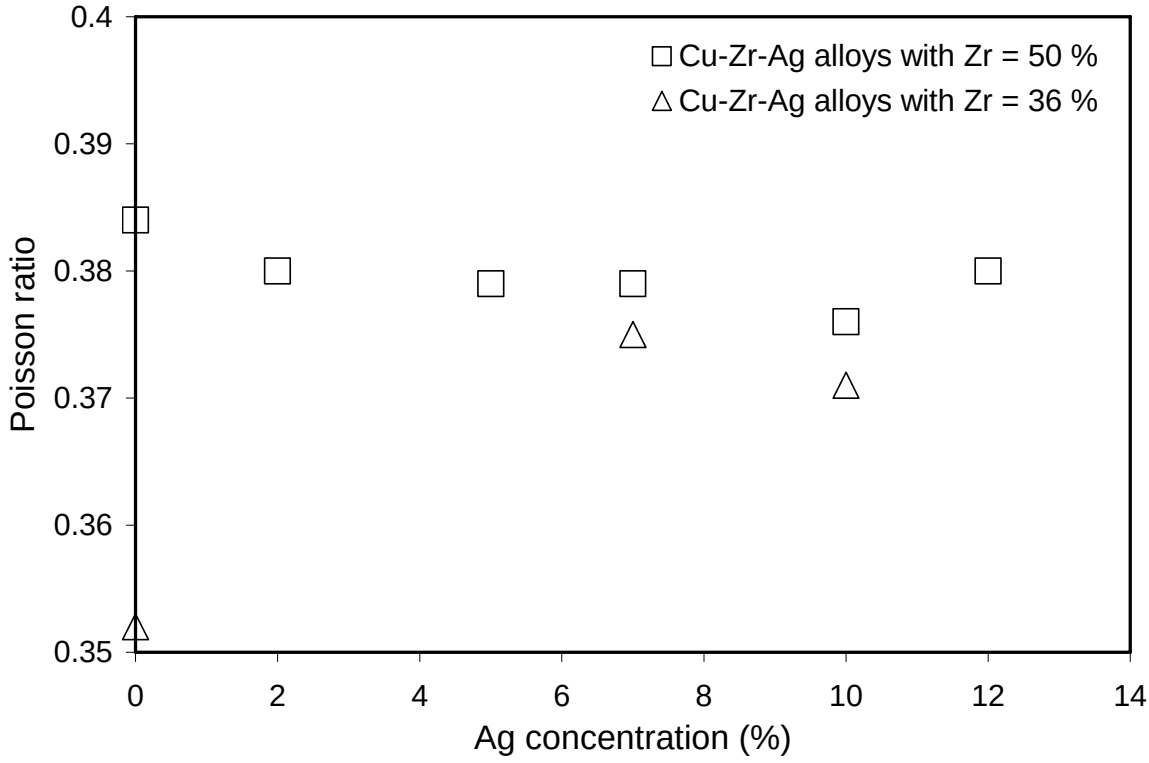

Figure 8.5. Poisson's ratio, ν, as a function of the Ag concentration for both $Cu_{(50-x)}Zr_{50}Ag_x$ and $Cu_{(64-x)}Zr_{36}Ag_x$ series.

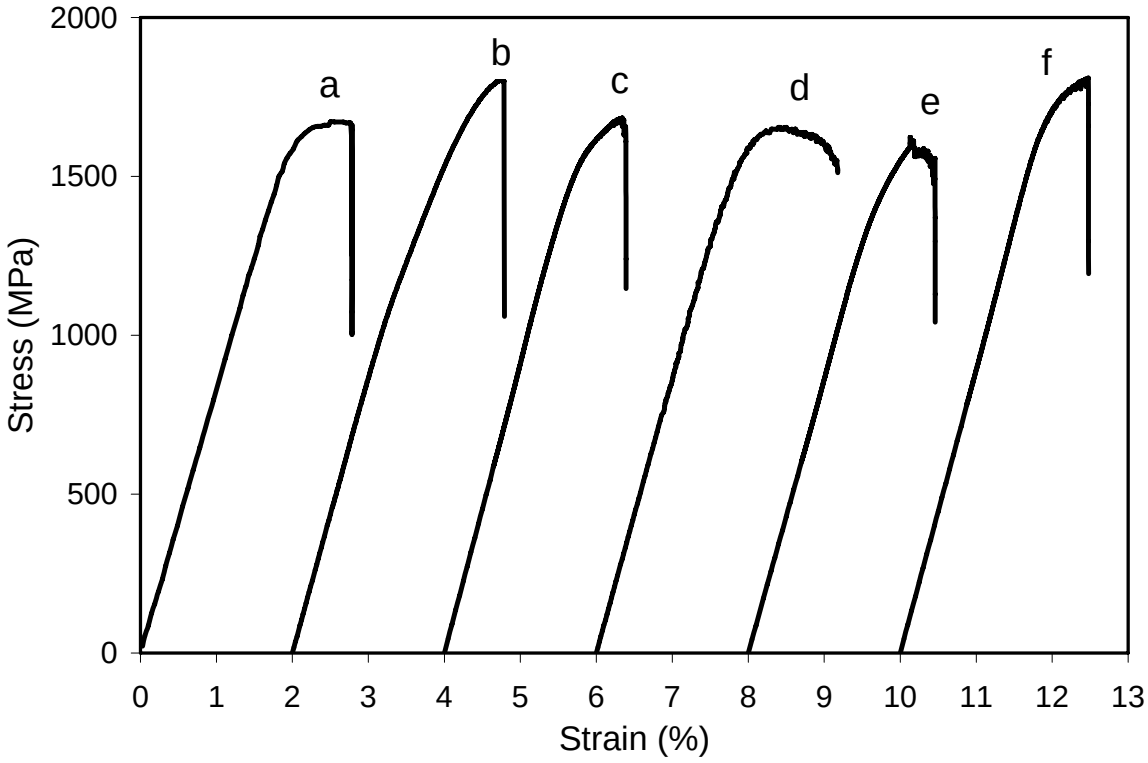

Figure 8.6. Compressive stress-strain curves of 2 mm amorphous rods for $Cu_{(50-x)}Zr_{50}Ag_x$ series alloys. (a), $Cu_{46}Zr_{54}$; (b), $Cu_{48}Zr_{50}Ag_2$; (c), $Cu_{43}Zr_{50}Ag_7$; (d), $Cu_{40}Zr_{50}Ag_{10}$; (e), $Cu_{38}Zr_{50}Ag_{12}$; and (f), $Cu_{43}Zr_{43}Ag_7Ti_7$.

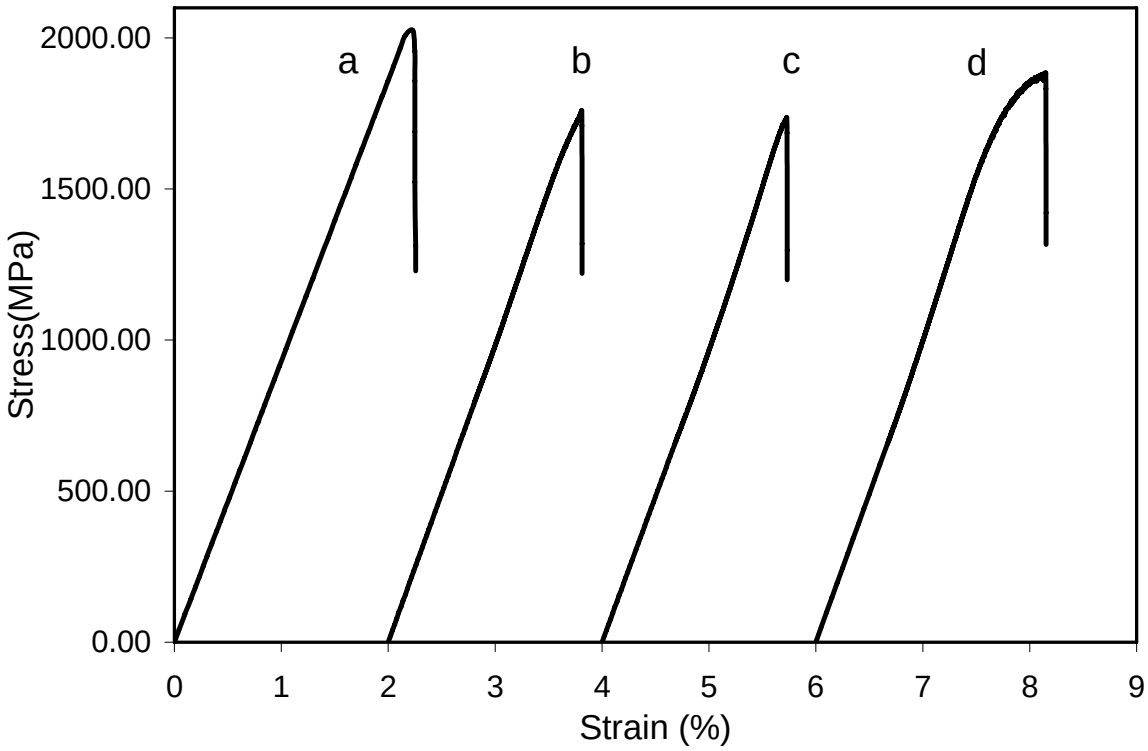

Figure 8.7. Compressive stress-strain curves of 2 mm amorphous rods for $Cu_{(64-x)}Zr_{36}Ag_x$ series alloys. (a), $Cu_{64}Zr_{36}$; (b), $Cu_{57}Zr_{36}Ag_7$; (c), $Cu_{54}Zr_{36}Ag_{10}$; and (d), $Cu_{40}Zr_{45}Ag_{10}Ti_5$.

It was recently found that in the Cu-Zr-Be alloy system, the shear modulus, G, and Poisson's ratio, ν, are very sensitive to changes in compositions. T_g and G decrease linearly with the increasing Zr concentration. Glasses with the same concentration of Zr and Ti show similar T_g and G [37]. In the present work, T_g of $Cu_{(50-x)}Zr_{50}Ag_x$ series does not vary much with changes in the Ag content. As a result, G and ν values are nearly constant. A T_g of ~ 670 K, a G of ~ 31.5 GPa, and a ν of ~ 0.380 are usually observed. Small variations may occur depending on the Ag content. Compared with the base alloy $Cu_{50}Zr_{50}$, $Cu_{(50-x)}Zr_{50}Ag_x$ alloys possess somewhat higher shear modulus, G, and bulk modulus, B. Consequently, ν of $Cu_{(50-x)}Zr_{50}Ag_x$ alloys does not deviate much from that of $Cu_{50}Zr_{50}$ (see Figure 8.5). However, in the $Cu_{(64-x)}Zr_{36}Ag_x$ series, Ag has a remarkable effect on reducing T_g. T_g is high for $Cu_{64}Zr_{36}$ (787 K), decreasing to 719 K as the Ag concentration increases to 10%, which is almost 70 K lower. G of $Cu_{57}Zr_{36}Ag_7$ and $Cu_{54}Zr_{36}Ag_{10}$ increases to 35.8 GPa and 35.2 GPa, respectively. B changes from 104.3 GPa for the binary $Cu_{64}Zr_{36}$ alloy to 130.5 GPa and 124.8 GPa for $Cu_{57}Zr_{36}Ag_7$ and $Cu_{54}Zr_{36}Ag_{10}$, respectively, resulting a significant increase in ν. Despite large differences in the absolute values of G and B for both $Cu_{(50-x)}Zr_{50}Ag_x$ and $Cu_{(64-x)}Zr_{36}Ag_x$ series, Poisson's ratios, ν, are very close.

Mechanical properties under a compressive applied load were measured on several 2 mm (diameter) by 4 mm (height) cylindrical specimens for each representative glassy alloy in both $Cu_{(50-x)}Zr_{50}Ag_x$ and $Cu_{(64-x)}Zr_{36}Ag_x$ series. It is found that $Cu_{(50-x)}Zr_{50}Ag_x$ series are ductile under compressive tests (see Figure 8.6). All the glassy alloys show high fracture strengths above 1.5 GPa and distinct plastic strains. For instance, $Cu_{54}Zr_{36}Ag_{10}$ glassy alloy exhibits fracture strength of ~ 1.55 GPa and plastic strain before failure ~ 1.4%, largest among this series of alloys. In comparison, for $Cu_{(64-x)}Zr_{36}Ag_x$ series alloys, although $Cu_{(64-}$

$_{x)}Zr_{36}Ag_x$ series exhibit high fracture strengths above 1.7 GPa, no apparent plastic deformations were observed (see Figure 8.7).

According to the recently developed Cooperative Shear Model, lower G implies that the shear flow barrier for an unstressed shear cooperative zone (SCZ) is relatively small, which allows the atoms to get into a higher potential energy configuration, and benefits the plastic yielding behavior. In the present Cu-Zr-Ag ternary glassy alloys, both $Cu_{(50-x)}Zr_{50}Ag_x$ and $Cu_{(64-x)}Zr_{36}Ag_x$ series show high Poisson's ratio ~ 0.375. However, $Cu_{(50-x)}Zr_{50}Ag_x$ alloys exhibit much lower G, which are ~ 31.5 GPa, than $Cu_{(64-x)}Zr_{36}Ag_x$ series. A G of ~ 35 GPa is usually found in $Cu_{(64-x)}Zr_{36}Ag_x$ series. Therefore, compressive plastic deformation observed in $Cu_{(50-x)}Zr_{50}Ag_x$ series can possibly be attributed to the lower/softer shear modulus.

8.4. Chapter Concluding Remarks

In summary, we started from the two binary bulk glass formers in the Cu-Zr system, and systematically investigated the compositional dependence of glass formation, thermal, elastic, and mechanical properties in the Cu-Zr-Ag ternary alloys. A good combination of high glass forming ability and high Poisson's ratio in both $Cu_{(50-x)}Zr_{50}Ag_x$ and $Cu_{(64-x)}Zr_{36}Ag_x$ series alloys was found. However, we only observed compressive plastic deformation in $Cu_{(50-x)}Zr_{50}Ag_x$ series. Using the recently developed Cooperative Shear Model, a possible interpretation is given.

References

[1] W. L. Johnson, Mrs Bulletin 24 (1999) 42.

[2] A. Inoue, Acta Materialia 48 (2000) 279.

[3] A. Peker, W. L. Johnson, Applied Physics Letters 63 (1993) 2342.

[4] V. Ponnambalam, S. J. Poon, G. J. Shiflet, Journal of Materials Research 19 (2004) 1320.

[5] V. Ponnambalam, S. J. Poon, G. J. Shiflet, Journal of Materials Research 19 (2004) 3046.

[6] F. Q. Guo, H. J. Wang, S. J. Poon, G. J. Shiflet, Applied Physics Letters 86 (2005) 091907.

[7] Z. P. Lu, C. T. Liu, J. R. Thompson, W. D. Porter, Physical Review Letters 92 (2004) 245503.

[8] D. H. Xu, G. Duan, W. L. Johnson, Physical Review Letters 92 (2004) 245504.

[9] F. Q. Guo, S. J. Poon, X. F. F. Gu, G. J. Shiflet, Scripta Materialia 56 (2007) 689.

[10] D. H. Xu, G. Duan, W. L. Johnson, C. Garland, Acta Materialia 52 (2004) 3493.

[11] D. H. Xu, B. Lohwongwatana, G. Duan, W. L. Johnson, C. Garland, Acta Materialia 52 (2004) 2621.

[12] G. Duan, D. H. Xu, W. L. Johnson, Metall. Mater. Trans. A 36A (2005) 455.

[13] A. J. Peker, W. L. Johnson, United States of America Patent 5288344 (1993).

[14] H. S. Chen, J. T. Krause, E. Coleman, Journal of Non-Crystalline Solids 18 (1975) 157.

[15] J. Schroers, W. L. Johnson, Physical Review Letters 93 (2004) 255506.

[16] X. J. Gu, A. G. McDermott, S. J. Poon, G. J. Shiflet, Applied Physics Letters 88 (2006) 211905.

[17] V. N. Novikov, A. P. Sokolov, Nature 431 (2004) 961.

[18] V. N. Novikov, A. P. Sokolov, Physical Review B 74 (2006) 064203.

[19] M. L. Lind, G. Duan, W. L. Johnson, Physical Review Letters 97 (2006) 015501.

[20] G. Duan, D. H. Xu, Q. Zhang, G. Y. Zhang, T. Cagin, W. L. Johnson, W. A. Goddard, Physical Review B 71 (2005) 224208.

[21] G. Duan, M. L. Lind, M. D. Demetriou, W. L. Johnson, W. A. Goddard, T. Cagin, K. Samwer, Applied Physics Letters 89 (2006) 151901.

[22] E. Bakke, R. Busch, W. L. Johnson, Applied Physics Letters 67 (1995) 3260.

[23] R. Busch, E. Bakke, W. L. Johnson, Acta Materialia 46 (1998) 4725.

[24] T. A. Waniuk, R. Busch, A. Masuhr, W. L. Johnson, Acta Materialia 46 (1998) 5229.

[25] D. C. Hofmann, G. Duan, W. L. Johnson, Scripta Materialia 54 (2006) 1117.

[26] G. J. Fan, M. Freels, H. Choo, P. K. Liaw, J. J. Z. Li, W. K. Rhim, W. L. Johnson, P. Yu, W. H. Wang, Applied Physics Letters 89 (2006) 241917.

[27] J. Das, M. B. Tang, K. B. Kim, R. Theissmann, F. Baier, W. H. Wang, J. Eckert, Physical Review Letters 94 (2005) 205501.

[28] A. Inoue, W. Zhang, T. Tsurui, A. R. Yavari, A. L. Greer, Philosophical Magazine Letters 85 (2005) 221.

[29] C. L. Dai, H. Guo, Y. Shen, Y. Li, E. Ma, J. Xu, Scripta Materialia 54 (2006) 1403.

[30] D. S. Sung, O. J. Kwon, E. Fleury, K. B. Kim, J. C. Lee, D. H. Kim, Y. C. Kim, Metals and Materials International 10 (2004) 575.

[31] E. S. Park, J. Y. Lee, D. H. Kim, Journal of Materials Research 20 (2005) 2379.

[32] Q. S. Zhang, W. Zhang, A. Inoue, Scripta Materialia 55 (2006) 711.

[33] E. S. Park, H. J. Chang, D. H. Kim, T. Ohkubo, K. Hono, Scripta Materialia 54 (2006) 1569.

[34] W. Zhang, A. Inoue, Journal of Materials Research 21 (2006) 234.

[35] W. Zhang, F. Jia, Q. S. Zhang, A. Inoue, Materials Science and Engineering a-Structural Materials Properties Microstructure and Processing 459 (2007) 330.

[36] A. A. Kundig, M. Ohnuma, T. Ohkubo, T. Abe, K. Hono, Scripta Materialia 55 (2006) 449.

[37] G. Duan, M. L. Lind, K. De Blauwe, A. Wiest, W. L. Johnson, Applied Physics Letters 90 (2007) 211901.